J Nanostruct 16(4): 5824-5834, Autumn 2026

RESEARCH PAPER

Fe_2O_3/MgO Nanosurface Doped Transparent Polymers: Analysis of Structural and Electronic Features for Photonic and Nanoelectronics Applications

Saba Razaq Salman [1], Ali S. Hasan [2], Abduljabar H. Ali [3], Mohammed A. Akraa [1], Ahmed Hashim [1], Ahmed F. Halbus [4], Zahraa H. Athab [5]*

[1] *Department of Physics, College of Education for Pure Sciences, University of Babylon, Babylon, Iraq*

[2] *Department of Polymer and Petrochemical Industries, College of Materials Engineering, University of Babylon, Babylon, Iraq*

[3] *Al-Bayan University, Baghdad, Iraq*

[4] *Department of Chemistry, College of Science, University of Babylon, Hilla, Iraq*

[5] *Environmental Research and Studies Center, University of Babylon, Hilla, Iraq*

ARTICLE INFO

Article History:
Received 06 June 2026
Accepted 24 September 2026
Published 01 October 2026

Keywords:
Electronic Characteristics
Fe_2O_3/MgO Nanosurface
Nanostructures
PVA

ABSTRACT

The current study was assigned to implement visualization for an innovative synthesis of magnesium oxide (MgO) and iron oxide (Fe_2O_3) as additives to the matrix polymer of polyvinyl alcohol (PVA). The nanostructures's investigation was based on methodological searching to improve their structural characteristics. The feedback revealed that the photoelectric features of the nanocomposite were boosted due to the incorporation of Fe_2O_3 and MgO nanostructures in the PVA. This occurred by reducing the bandgap of PMA matrix polymer from 4.215 to 2.914 eV by adding both Fe_2O_3 and MgO nanoparticles, along with other promising electronics parameters enhancement. The study presents compelling evidence that the PVA/Fe_2O_3/MgO nanostructure exhibits outstanding electronic properties. This finding underscores its considerable potential for applications in the fields of nanoelectronics and photonics.

How to cite this article
Razaq Salman S., Hasan A., Ali A. Fe_2O_3/MgO Nanosurface Doped Transparent Polymers: Analysis of Structural and Electronic Features for Photonic and Nanoelectronics Applications. J Nanostruct, 2026; 16(4):5824-5834. DOI: 10.22052/JNS.2026.04.111

INTRODUCTION

The composite containing a matrix polymer with nanoparticle additives is called polymer nanocomposite materials (PNCMs). The added nanoparticles are non-organic and are evenly dispersed throughout the matrix polymer. This description grants material an attractive interest for scientists as effective tools to evolve numerous instruments for diverse applications. The hybrid attributes of the PNCMs grant a wide spectrum of usages, which serve human life requirements. The additives back up the fields of energy, electronics, optics, and sensors. The role of PNCMs appears to be due to the considerable enhancement of pyro-physical characteristics attributed to the presence of nanoparticles [1]. The synthetic PVA consists of linear carbon chains with functional groups of hydroxyl, resulting in a semi-crystalline structure. Polymers according to this chemical description are water-soluble,

* *Corresponding Author Email: pure.saba.rasaq@uobabylon.edu.iq*

This work is licensed under the Creative Commons Attribution 4.0 International License.
To view a copy of this license, visit http://creativecommons.org/licenses/by/4.0/.

accessible, thermally stable, and have excellent film-forming properties [2]. Magnesium oxide (MgO)'s features such as considerable hardness, elevated purity, non-odorous, non-toxicity, and high thermal stability ensure that it is an effective component of PNCMs [3]. The significance of MgO as a promising candidate is attributed to its reduced thermal conductivity. Furthermore, several potential applications of MgO are based on its optical, chemical, and thermal properties [4, 5]. Iron oxide (Fe_2O_3) behaves as a semiconductor material with a low band gap of 2.2 eV and promotes thermodynamic equilibrium. In addition to the presented properties, they introduce it as a compelling nominee for various optical applications [5, 6]. The Fe_2O_3 manifests non-toxicity, a reduced impurity abundance, and a prominent natural multitude [7, 8]. The integration of metal oxides into polymers is a key area of interest for researchers aiming to enhance the material's electronic, electrical, and optical characteristics [9-11]. Within the framework of seeking an innovative nanostructure consisting of metal oxides and polymers, the current work concentrates on designing the nanocomposite PVA/Fe_2O_3/MgO as a novel resolution to fulfill the requirements of the industrial problems.

QUANTUM COMPUTATIONAL METHODS

To identify the targeted molecular electronic and vibrational characteristics, the quantum computations were achieved through the Gaussian 09W software package. The execution was on the platform of an Intel Core i9 processor, the graphic card of an AMD Radeon Pro 5500M, and the RAM of 32 GB [12-14]. The computations of the molecular characteristics were optimized by modifying the molecular structure as a first step before invoking the framework of time-dependent density functional theory (TD-DFT) through B3LYP hybrid functional [15, 16]. Becke and Lee et al. proposed a functional that combines Becke's three-parameter functional with a Hartree-Fock exchange contribution, while also include nonlocal corrections for both the exchange potential and correlation energy. The B3LYP method is preferred for its accuracy and computational efficiency compared to ab initio methods [17, 18]. A comprehensive set of property calculations was carried out using the 6-31G (d,p) basis set. The calculated properties include total energy, frontier molecular orbital energies (HOMO and LUMO), ionization energy, band gap, electron affinity, electronegativity, chemical hardness, chemical softness, electrophilicity, dipole moment, harmonic vibration frequency, and optimized geometry [19, 20]. According to this approach of calculating the electron correlation assessment, the term of exchange-correlation (EKC) within the TD-DFT method was employed, which encompasses the contributions of the exchange energy and the dynamic correlation [21, 22]. The considered molecules are depicted in Fig. 1. Within the TD-DFT framework, the electronic energy can be dissected into distinct components, as articulated in Eq. 1:

$$E = E_T + E_V + E_J + E_{KC} \quad (1)$$

In this context, ET denotes the electronic kinetic energy, EV signifies the energy arising from electron-nuclear attraction, EJ represents the energy originating from electron-electron repulsion, and EKC corresponds to the exchange-correlation term, which serves to account for electron correlation effects within the TD-DFT framework. The ionization potential (IP) serves as a quantification of the energy requisite for the removal of one or more electrons from a neutral molecule, leading to the formation of a positively charged ion. Eq. 2 articulates the ionization potential as the energy disparity between the energy of the cationic state and the energy of the neutral molecule.

$$IP = Ecation–En \quad (2)$$

On the other hand, electron affinity (EA) measures the tendency of a neutral molecule to resist the loss of electrons. Eq. 3 calculates the electron affinity as the energy difference between the neutral molecule and the corresponding anionic state.

$$EA = En - Eanion \quad (3)$$

Within the context of TDDFT, two important global quantities are the chemical potential (μ and electronegativity (χ) (Eq. 4). The ground-state electronic energy ((N)) of a system, which depends on the number of electrons (N), is used to define these quantities. The derivative of (N) with respect to N at a constant external potential (r) gives the chemical potential or the negative of the absolute

CC BY

electronegativity [23-25].

$$\mu \approx \left(\frac{\partial z}{\partial N}\right)_{v(\vec{r})} \approx -\chi \quad (4)$$

Chemical hardness, defined within TDDFT, is the second derivative of the electronic energy with respect to the number of electrons N at a constant external potential (r) [26-28]. It quantifies the resistance of the chemical potential to changes in the number of electrons (Eq. 5).

$$\eta = \frac{1}{2}\left(\frac{\partial^2 E}{\partial N^2}\right)_{v(\vec{r})} = \frac{1}{2}\left(\frac{\partial \mu}{\partial N}\right)_{v(\vec{r})} \quad (5)$$

Engaging in calculating the electronic characteristics entails employing one out of two methods. The first is the energy-vertical method, which includes the application of the finite difference approximations on the discrepancies of the total electronic energies due to the addition or removal of electrons from the neutral molecule. The second method is the orbital-vertical method that deals with the (HOMO) and (LUMO) energy levels of the neutral molecule, Koopmann theorem [18]. Through finite difference approximations, the expressions for the determination of electronegativity (χ) and chemical hardness (ŋ) can be formulated as [29, 30]:

$$\chi = (IP + EA)/2 \quad (6)$$

$$\eta = (IP - EA)/2 \quad (7)$$

Alternatively, using Koopman's theorem, these equations can be rewritten as:

$$\chi = (E_{HOMO} + E_{LUMO})/2 \quad (8)$$

$$\eta = (E_{HOMO} - E_{LUMO})/2 \quad (9)$$

The chemical softness quantity appears as the feature of the chemical reactivity degree, which is opposite to the chemical hardness property. The higher the value of the chemical softness, the lower the value of the chemical hardness. This evidences the alteration absence of energy, which links to the disproportionation reaction [31, 32].

$$S = \frac{1}{2\eta}\left(\frac{\partial^2 N}{\partial E^2}\right)_{v(\vec{r})} = \frac{1}{2}\left(\frac{\partial N}{\partial \mu}\right)_{v(\vec{r})} \quad (10)$$

The measurement of a chemical species's reduced energy is referred to as electrophilicity (w), which indicates the maximum flow of electrons between a donor and an acceptor. It is defined as [21, 22]:

$$\omega = \mu^2/2\eta \quad (11)$$

RESULTS AND DISCUSSION

The research sought to ameliorate the structure of the polymer matrix (PVA) through the inclusion of the nanoparticles of (Fe_2O_3/MgO) for reaching the optimum electronic features of the produced nanocomposite (PVA/Fe_2O_3/MgO). The findings were obtained from the processing of the software of the Gaussian 09 programs and simultaneously, the method of the Time-Dependent Density Functional Theory (TDDFT). The results are shown in Figs. 1 and 2, which depict the most favorable arrangement of the geometrical positions of molecules [33]. The outcomes supported the accuracy of the work by providing insights into the nanostructure's electronic properties. Additionally, the mentioned methods contributed effectively to identify the molecular structure. Furthermore, they connect the experimental results with the optimized theoretical calculation.

Figs. 1, and 2 show the considered material chemical groups. The deduced bond of (C-C) of 1.52 Å evidences the presence of the double bonds. Additionally, a carbonyl group of 1.422 Å is found as well. While the length of 1.431 Å indicates the bond of carbon-oxygen (C-O) bond. This description aligns with the ideal bond lengths encountered in the aromatic rings [34, 35]. Additionally, the length of the C-H bond was 1.091 Å throughout the study, despite potential influences such as electrostatic interactions and hydrogen bonding with molecular forces. Furthermore, during chemical reactions, transient deviations from equilibrium bond lengths can arise due to transitional states, reaction pathways, activation energies, and intermediate states [36, 37].

Regarding the complexes, the length of the bonds, Fe-O, and Mg-O, were 1.92 Å and 2.013 Å, respectively. The bond length corresponds to the noted standard values in the symmetric systems. That refers to the reactions producing the Fe_2O_3, and MgO enclosed by the structures of the composite.

The interaction between Fe_2O_3/MgO and PVA

CC BY

is mutually effective. This results in Fe_2O_3/MgO being integrated into the nanocomposite, creating a favorable environment for nanoparticles-PVA interaction. These metal oxides may assume the role of catalysts or initiators, thereby facilitating chemical transformations within the polymer matrix. This synergy opens up prospects for shared applications or the development of composite compositions that can capitalize on the synergistic interactions between these materials [38, 39]. It becomes evident that post-relaxation occurs as a substantial transformation in the conformation of the PVA chain. This structural modification implies that PVA and the Fe_2O_3/MgO compound, presumably constituting another composite, participate in intermolecular interactions, such as van der Waals forces, hydrogen bonds, or stacking interaction. These interactions promote the alignment and aggregation of the polymer chains with the composite, ultimately leading to the formation of novel structures or phases within the composite material [40].

Table 1 provides an extensive compilation of findings emanating from ground state calculations applied to the polymeric composites within this study, with a specific emphasis on ascertaining configurations that minimize energy. This comprehensive analysis encompasses several critical parameters, as a Total Energy (ET, in atomic units, a.u.). This parameter offers a holistic

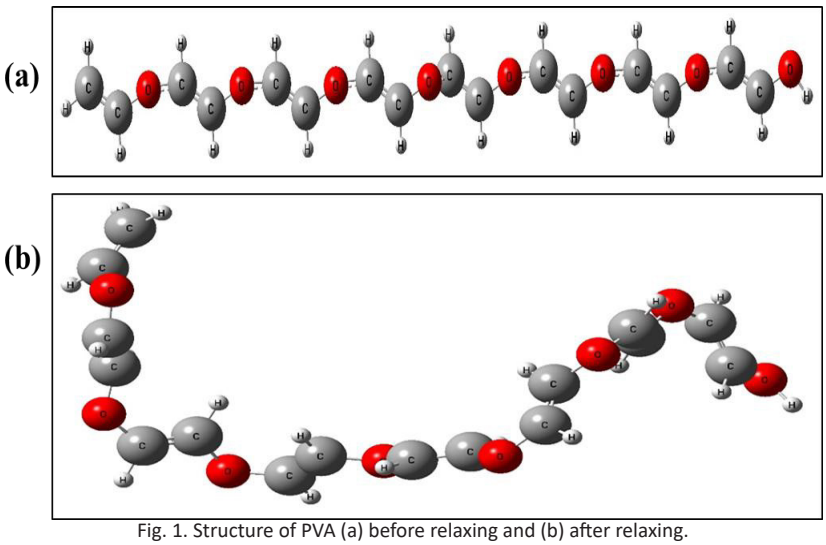


Fig. 1. Structure of PVA (a) before relaxing and (b) after relaxing.

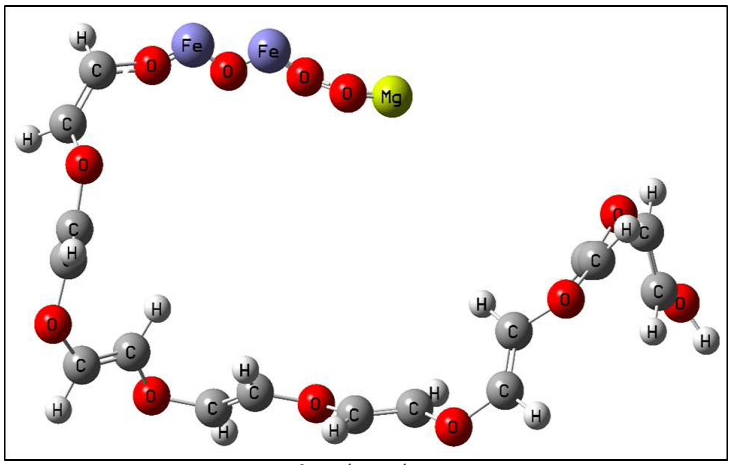


Fig. 2. Structure of PVA/Fe_2O_3/MgO nanostructures

CC BY

measure of the system's energy, facilitating comparisons across various configurations of the polymeric composites. Ionization Potential (IP) and Electron Affinity (EA): These parameters, determined through Koopman's theorem and expressed in electron volts (eV), offer insights into the composite's electronic characteristics. Also, Electronegativity (χ) and Chemical Potential (μ, in eV) exhibit an inverse relationship, where an enhancement in electronegativity corresponds to a reduction in chemical potential. Chemical hardness (η), chemical softness (S), electrophilicity (ω), and energy gap (Eg) were calculated. The contrast between the levels of (HOMO) and (LUMO) represents the conductivity measure of the material. The potential for electronic applications, electrostatic potential (ESP) surfaces, and 3-D electron density (TD) relies on the physical quantity of conductivity.

The computations revealed the dielectric properties of the Fe_2O_3/MgO nanoparticles into the PVA matrix. The interaction among the components of the nanocomponent enhances the total energy (ET) in the system. The synergistic impact of the electrostatic interaction and chemical bonding boosts the nanostructure's total energy. The incorporation of the nanoparticles into the polymer matrix requires breaking the original bonds of the polymer and creating novel bonds among nanoparticles and the surrounding polymer matrix [11, 18, 41]. Incorporating the Fe_2O_3/MgO within the polymer matrix elevates the mechanical properties, involving the tensile strength and elasticity modulus. Developing mechanical properties qualifies material for vast applications of high mechanical quality such as aerospace constructures, automotive parts, and sports appliances. Additionally, Fe_2O_3 unveils magnetic features for the nanocomposite, yielding appropriate matter for applying magnetic sensors, electromagnetic shielding, and data loading apparatuses [9, 42, 43]. Regarding the data in Table 1, the PVA/Fe_2O_3/MgO nanocomposite's values of ionization potential (IP) and electron affinity (EA) are superior to those of the PVA matrix. The heightened IP refers to the tendency to retain the electron while raising the EA represents a sign of the attractive potential for more additional electrons. Variations in the chemical composition, bonding characteristics, and structure of composites lead to differences in their electronic features. The presence of foreign nanoparticles (Fe_2O_3 and MgO) creates exceptional groups with electron-accepting or donating abilities. Consequently, this reconfigures the entire electronic composite's conduct. Moreover, the chemical alterations of the ambient like the metallic ions transition or the configurations of distinguishable bonding can impact IP and EA values. These extra elements are known for their general effective change in electronic behavior [19, 44, 45]. The chemical potential (μ) and electronegativity (χ) are correlated and inversely proportional. As the value of electronegativity (χ) increases, the ability of an atom to attract electrons becomes stronger. Therefore, all thermodynamic properties of the atoms in a system, as well as their electronic behavior, are influenced by the differences in their electronegativity (χ). The findings indicate that the addition of Fe_2O_3/MgO to the nanocomposite enhances the chemical softness (S) and electrophilicity (ω) values of PVA/Fe_2O_3/MgO, while reduce the chemical hardness (η). The addition of nanoparticles modifies the structure of the polymer matrix, reshaping the energy levels and the distribution of electronic states. The alterations activate a chemical reaction in the material by using Fe_2O_3/MgO as sources of electron donors or acceptors. This influences the electronic characteristics and facilitates electron processes. All changes in electronic properties, which include softness, electrophilicity, and chemical hardness, enhance the material's mechanical properties, such as ductility, processability, flexibility, and overall stability [20, 46-48]. The Fe_2O_3/MgO decline the band gap (Eg) of the matrix polymer, or in other words, reduce the difference of energy between the LUMO and HOMO levels. The alteration of the electronic configuration stems from several mechanisms, including the chemical bonds, electrostatic interactions, and the intermolecular

Table 1. The role of TD-DFT B3LYP/6-31(d,p) in revealing the electronic features of polymeric composites.

Sample	E_T	HOMO	LUMO	E_g	IP	EA	χ	μ	η	S	ω
PVA	-8421.325	-7.2365	-3.0214	4.215	7.237	3.021	5.129	-5.12	2.108	0.237	6.241
PVA/Fe_2O_3/MgO	-5876.985	-7.5463	-4.6321	2.914	7.546	4.632	6.089	-6.08	1.457	0.343	12.723

CC BY

binding force between the Fe_2O_3/MgO and PVA. Novel electronic states accompany the modified electronic structure of the nanocomposite. The formed covalent or ionic bond due to the added Fe_2O_3/MgO affected the latter [4, 49, 50]

The latter adds new energy levels to the polymer electronic construction. Furthermore, the nanoparticles influence the distribution of

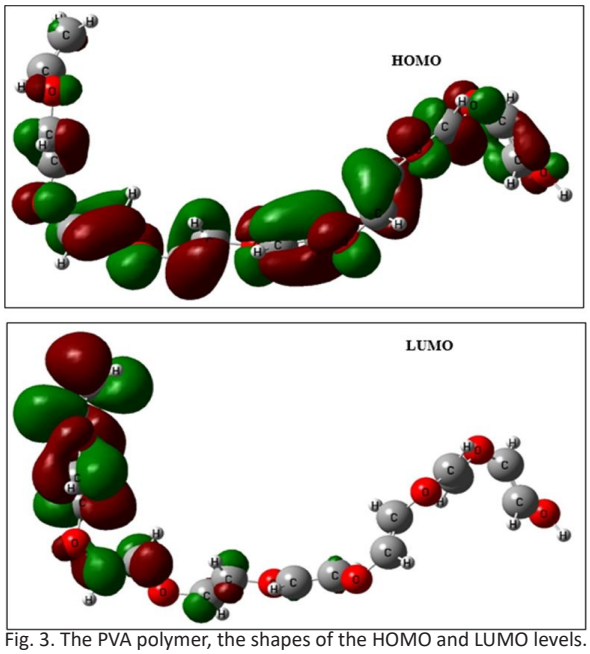


Fig. 3. The PVA polymer, the shapes of the HOMO and LUMO levels.

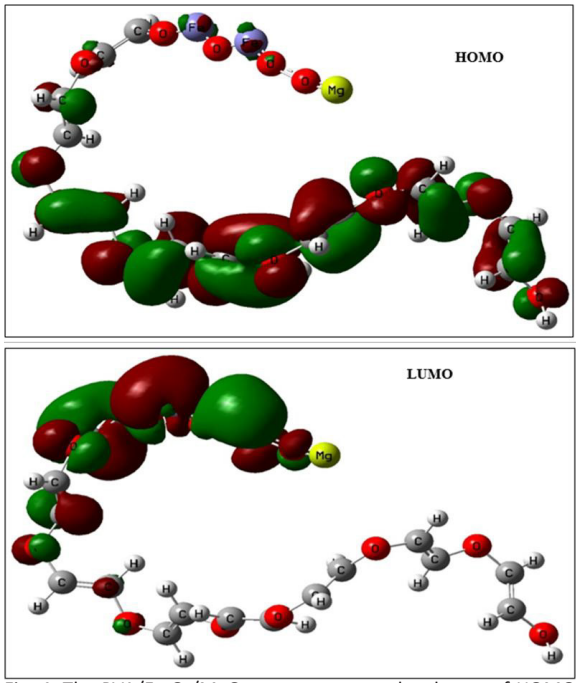


Fig. 4. The PVA/Fe_2O_3/MgO nanostructures, the shapes of HOMO and LUMO levels.

CC BY

electron density and polarization within the nanocomposite by altering the electric field and the surroundings of the polymer chains, which gives rise to new energy states within the electronic band structure [35, 51].

The energy levels of the PVA/Fe_2O_3/MgO nanostructures are illustrated in Figs. 3 and 4. These Figures show a more stable distribution of electrons compared to that of pure PVA polymer. This behavior can be attributed to the electron-withdrawing properties of the Fe_2O_3 and MgO nanoparticles. The superiority of transition metal oxides's electron affinity compared to that of PVA indicates a strong attraction for electrons. This phenomenon leads to a redistribution of the electron density within the system. The redistribution of electrons enhances the stability of the electronic system by reducing disordered localized charges and the regions of concentrated electrons within the polymer [6, 52, 53]. System instability within a material arises from the surrounding spatial charge imbalances, which leads to effective electrostatic repulsion. Electron redistribution that achieves charge balance results in localized charge accumulation reaching a mitigated state. Promoting a more uniform distribution minimizes the repulsive forces, thereby enhancing electronic stability [12, 54, 55].

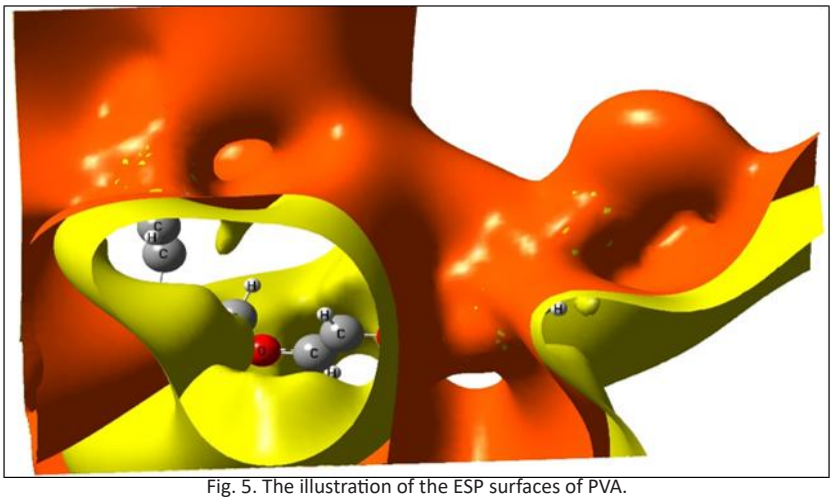


Fig. 5. The illustration of the ESP surfaces of PVA.

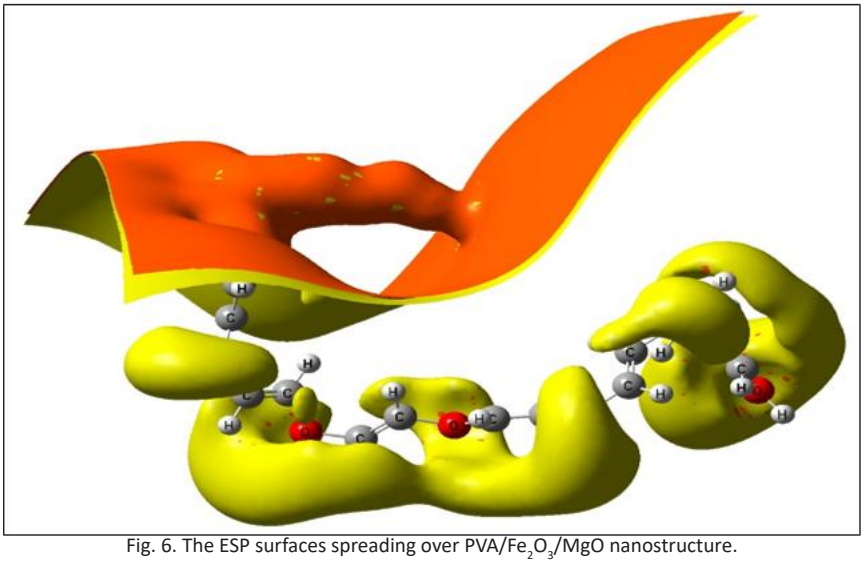


Fig. 6. The ESP surfaces spreading over PVA/Fe_2O_3/MgO nanostructure.

CC BY

The electrostatic potential (ESP) surfaces for both PVA and the PVA/Fe_2O_3/MgO composite are illustrated in Figs. 5 and 6, respectively. The two systems are clearly distinguished by their different colors. The presence of the nanoparticles, Fe_2O_3 and MgO, alters the ESP topography, especially in their immediate vicinity, due to their unique surface chemistries compared to the PVA matrix. This results in noticeable differences in the ESP distribution configurations, particularly in areas of higher potential, across the surfaces of both systems [24, 56]. The ESP distribution is one of the most effective alterations, which occurs by adding the Fe_2O_3/MgO in the PVA matrix. This transformation appears as distinguished chromatic disparity and attractive surface of nanocomposite for the negative charges [5, 57]. The influence described here depends on the type of charge carried by the nanoparticle. For example, the negative charge of Fe_2O_3 attracts

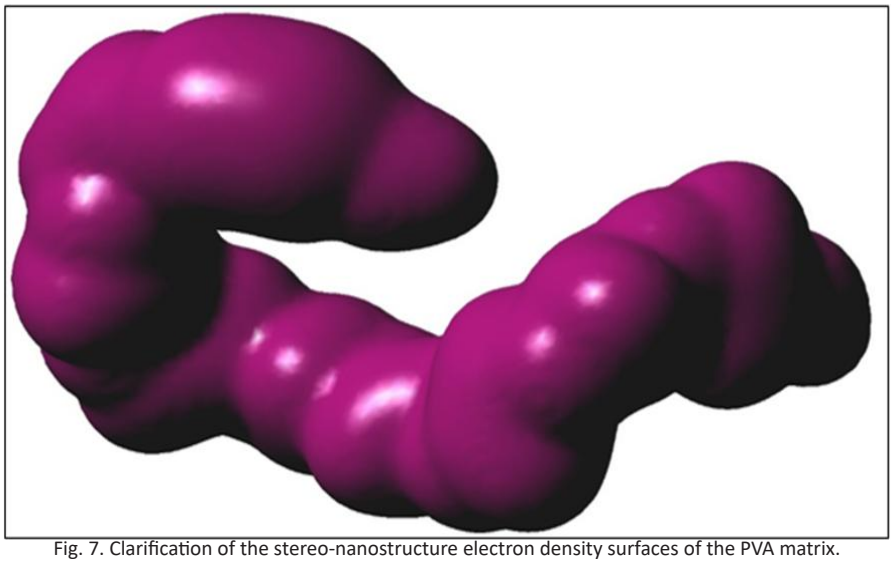


Fig. 7. Clarification of the stereo-nanostructure electron density surfaces of the PVA matrix.

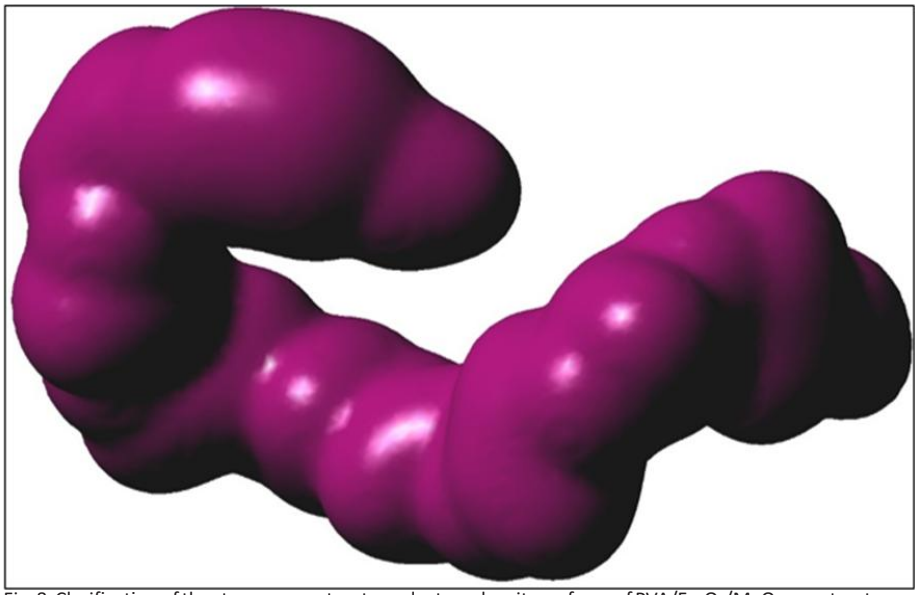


Fig. 8. Clarification of the stereo-nanostructure electron density surfaces of PVA/Fe_2O_3/MgO nanostructures.

CC BY

positive charges from the surrounding area, resulting in a redistribution of electrical potential. The interaction between the added nanoparticles and the polymer chains results in the formation of induced dipoles. This dipole formation occurs between the nanoparticles and the polymer chains, leading to a complex rearrangement of charges and modifications to the local electrostatic potentials. The polarization concentration is located at the interface between the polymer and particles of metal oxides [58].

The Fe_2O_3 and MgO influenced the electron density distribution for their differences in shape, size, and electron densities. The three-dimensional electron density (TD) is revealed obviously in Figs. 7 and 8, for the polymer matrix and nanocomposite, respectively. The high density of the Fe_2O_3 and MgO enhanced the electron density in the PVA/Fe_2O_3/MgO nanostructure. The closeness of the Fe_2O_3 and MgO to each other exaggerates this effect [34]. The Fe_2O_3 and MgO can be considered a polarization catalyst that impacts its surroundings by transferring the charge. The interaction between the nanoparticles and the PVA matrix increases the electron density at the interface, thus redistributing the electrons. This unique behavior produces a novel nanocomposite [13, 55, 59].

CONCLUSION

This research demonstrated a design of PVA/Fe_2O_3/MgO nanostructures that is suitable for electronic and photonic applications. The findings played a successful role in the modification of the PVA molecular structure, such that decreased the band gap of PVA from 4.215 to 2.914 eV. The findings highlight the exceptional electronic properties of PVA/Fe_2O_3/MgO. These enhanced features position the nanostructure for a wider range of applications.

ACKNOWLEDGMENTS

Thanks to the University of Babylon.

CONFLICT OF INTEREST

The authors declare that there is no conflict of interests regarding the publication of this manuscript.

REFERENCES

1. Bafna M, Deeba F, Gupta AK, Shrivastava K, Kulshrestha V, Jain A. Analysis of Dielectric Parameters of Fe_2O_3-Doped Polyvinylidene Fluoride/Poly(methyl methacrylate) Blend Composites. Molecules. 2023;28(15):5722.
2. Olvera Bernal RA, Olekhnovich RO, Uspenskaya MV. Chitosan/PVA Nanofibers as Potential Material for the Development of Soft Actuators. Polymers. 2023;15(9):2037.
3. Bharati B, Vijaykumar BT, Ramabai N, Basavaraj S. Synthesis, characterizations, and physical properties of magnesium oxide with polyaniline nanocomposites. Materials Today: Proceedings. 2023;92:1640-1645.
4. Khalil KD, Bashal AH, Khalafalla M, Zaki AA. Synthesis, structural, dielectric and optical properties of chitosan-MgO nanocomposite. Journal of Taibah University for Science. 2020;14(1):975-983.
5. Tewatia K, Sharma A, Kumar A, Kumar K, Sowjanya Pali L, Lal S. Enhanced optical properties of recycled Fe_2O_3 reinforced in PVDF nanocomposite thin films for energy harvesting. Materials Today: Proceedings. 2023;94:39-43.
6. Rasheed F, Salah A, Kazem A. Studying the Optical and Morphology Properties of PMMA and $Batio_3$/Sb_2O_3 PMMA Hybrid Nanoparticles Coatings Doped for Application Coatings Solar Cells and Electronic Screen. System Safety: Human - Technical Facility - Environment. 2025;7(1):465-481.
7. Abdulkareem HI, Braihi AJ, Hasan AS. Smart behaviors of thermochromic materials: A review. AIP Conference Proceedings: AIP Publishing; 2026. p. 070009.
8. Zhuang Y, Shi B. Polymer hydrogels with enhanced stability and heterogeneous Fenton activity in organic pollutant removal. Journal of Environmental Sciences. 2019;85:147-155.
9. Dhyool MT, Alobad ZK, Hassan AS. Tailoring Epoxy Nanocoatings for Enhanced Light Reflectance and Mechanical Properties Using Metal Oxide Nanoparticles. Revue des composites et des matériaux avancés. 2026;36(2):349-362.
10. Fadil OB, Hashim A. Fabrication and Tailored Optical Characteristics of CeO_2/SiO_2 Nanostructures Doped PMMA for Electronics and Optics Fields. Silicon. 2022;14(15):9845-9852.
11. Son Y-W, Cohen ML, Louie SG. Half-metallic graphene nanoribbons. Nature. 2006;444(7117):347-349.
12. Kadhim MH, Hasan AS, Akraa MA, Layla AY. Preparation and optimization of heterojunction donor(DLC) – acceptor(SI) as a solar cell by DFT and PLD. Journal of Ovonic Research. 2021;17(3):273-281.
13. Elgharbawy AS, El Demerdash A-GM, Sadik WA, Kasaby MA, Lotfy AH, Osman AI. Synthetic Degradable Polyvinyl Alcohol Polymer and Its Blends with Starch and Cellulose—A Comprehensive Overview. Polymers. 2024;16(10):1356.
14. Abdulimam M, Hamzah A, Hasan A. Numerical Investigation for Bending Behavior of Hybrid Core Composite Sandwich Structure. System Safety: Human - Technical Facility - Environment. 2025;7(1):396-405.
15. Chemical Recycling of Polystyrene to Valuable Chemicals via Selective Acid-Catalyzed Aerobic Oxidation under Visible Light. American Chemical Society (ACS). http://dx.doi.org/10.1021/jacs.2c01410.s001
16. Hasan AS, Hassan HB, Hashim A. Synthesis and unraveling the optical and electronic characteristics of PVA/Co_2O_3/Fe_2O_3 hybrid nanostructures for promising nanoelectronics and photonics applications. Optical and Quantum Electronics. 2024;56(4).
17. Rajesh T, Sailaja DBBV. Metal Oxide Nanoparticles As Antimicrobial Agents: Sol-Gel Synthesis And Activity Against

CC BY

Agriculturally Important Bacterial Pathogens. Journal of Applied Bioanalysis. 2025;11(s9).
18. Habeeb Rahiman K, Unnikrishnan G, Sujith A, Radhakrishnan CK. Cure characteristics and mechanical properties of styrene–butadiene rubber/acrylonitrile butadiene rubber. Mater Lett. 2005;59(6):633-639.
19. Chantawansri TL, Sirk TW, Byrd EFC, Andzelm JW, Rice BM. Shock Hugoniot calculations of polymers using quantum mechanics and molecular dynamics. The Journal of Chemical Physics. 2012;137(20).
20. Mohammed FQ, Edan MS, Hasan AS, Haider AJ. Synthesis and Theoretical Concepts of Boron Nitride Nanowires Grown on Nitrides Stainless Steel Surface by Hybrid Gas Phase Process. Key Eng Mater. 2021;886:97-107.
21. Abud SH, Hasan AS, Almaamori M, Bayan N. Enhancement the ability to pump crude oil using rubber solutions. Journal of Physics: Conference Series. 2021;1818(1):012235.
22. Johnston K, Harmandaris V. Properties of short polystyrene chains confined between two gold surfaces through a combined density functional theory and classical molecular dynamics approach. Soft Matter. 2012;8(23):6320.
23. Design, Optimization, Structural and Electronic Properties of PVA/ZnO/SnO_2 Nanostructures for Nanoelectronics Fields. Nanosistemi, Nanomateriali, Nanotehnologii. 2024;22(3).
24. Zhang L, Zhao J, Zhu J, He C, Wang H. Anisotropic tough poly(vinyl alcohol) hydrogels. Soft Matter. 2012;8(40):10439.
25. Bala V, Sharma M, Tripathi SK, Kumar R. Investigations of Al:CdS/PVA nanocomposites: A joint theoretical and experimental approach. Materials Chemistry and Physics. 2014;146(3):523-530.
26. Design and Exploring the Structure and Electronic Characteristics of PS/MnO_2/NiO Nanosystem for Optics and Electronics Nanodevices. Nanosistemi, Nanomateriali, Nanotehnologii. 2024;22(3).
27. Maharani EP, Triwitono P, Pranoto Y, Marseno DW. Polyvinyl Alcohol/ Cinnamon Essential Oils-Loaded Porous Rice Starch Composite Film for Active Food Packaging with Slow Release. Advances in Science and Technology; 2026/06/19: Trans Tech Publications Ltd; 2026. p. 23-30.
28. Mohammed FQ, Hasan AS, Musafir MAA. Performance Optimization for Mechanical Properties and Corrosion Resistance of Mg-Al Rolled Alloy with Zn Nano-Coating. Journal of Applied Research and Technology. 2026;24(1):75-82.
29. Sawant M, Chakraborty T, Yadav D, Biranje S, Saxena S, Shukla S. Stabilization strategies and optimization of polyvinyl alcohol-chitosan hybrid polymer. Hybrid Advances. 2025;8:100345.
30. Gao Q, Wang M, Kang X, Zhu C, Ge M. Continuous wet-spinning of flexible and water-stable conductive PEDOT: PSS/PVA composite fibers for wearable sensors. Composites Communications. 2020;17:134-140.
31. Fitriani F, Aprilia S, Mahardika M, Masruchin N, Rinaldi W. Development of hybrid biodegradable polymer based on polyvinyl alcohol and whey protein isolate reinforced with cellulose nanocrystal from pineapple crown leaf. Case Studies in Chemical and Environmental Engineering. 2025;11:101061.
32. A. Akraa M, Hasan AS, Kadhim MJH. Spectroscopy Characterization of Ethylene Vinyl Acetate Degradation by Different Kinds of Accelerated Aging. Baghdad Science Journal. 2020;17(3).
33. Cibilakshmi G, Jegan J. A DOE approach to optimize the strength properties of concrete incorporated with different ratios of PVA fibre and nano-Fe_2O_3. Advanced Composites Letters. 2020;29.
34. Jebur SK, Braihi AJ, Hassan AS. Graphene effects on the structural, morphological and optical properties of PEDOT:PSS thin films. Materials Today: Proceedings. 2022;49:2733-2740.
35. Hasan AS, Kadhim MJH, Layla AY, Al-Khafaji Z. Exploring the NiPcTs-Si nanoheterojunction as a bilayer solar cell: theoretical and experimental analysis. Optical and Quantum Electronics. 2024;56(11).
36. Hou R, Zhang G, Du G, Zhan D, Cong Y, Cheng Y, et al. Magnetic nanohydroxyapatite/PVA composite hydrogels for promoted osteoblast adhesion and proliferation. Colloids Surf B Biointerfaces. 2013;103:318-325.
37. Hasan AS, Mousa AH, Hussein ARA. Molecular Dynamics Simulation of SWCNT / PYA in sensors application. 2022 Muthanna International Conference on Engineering Science and Technology (MICEST); 2022/03/16: IEEE; 2022. p. 83-88.
38. Al-Abass SFA, Braihi AJ, Hasan AS. Oil spill cleaning up by polymeric sorbents using salt leaching method. AIP Conference Proceedings: AIP Publishing; 2023. p. 020024.
39. Abdulkareem HI, Braihi AJ, Hasan AS. EFFECT OF SURFACTANT TYPE AND AMOUNT ON THE THERMOCHROMIC PROPERTIES OF POLYDIACETYLENE. Kufa Journal of Engineering. 2025;16(4):475-493.
40. Luan X, Younse H, Hong H, Peterson GP. Improving mechanical properties of PVA based nano composite using aligned single-wall carbon nanotubes. Materials Research Express. 2019;6(10):1050a1056.
41. Al-Kawaz YAE, Braihi AJ, Hasan AS. Polymeric and Hybrid Membranes for Achieving Ultra-Low Sulfur Fuel Requirements. Revue des composites et des matériaux avancés. 2025;35(6).
42. Al-Maamori MH, Al-Jamal AN, Habeeb SA, Hassan AS, Majdi HS. Al^{3+} -modified ZnO thin film sensor fabricated by the sputtering method: Characterization and a carbon monoxide gas detection study. Journal of Chemical Research. 2024;48(1).
43. Iqbal T, Irfan M, Ramay SM, Mahmood A, Saleem M, Siddiqi SA. ZnO–PVA Polymer Matrix with Transition Metals Oxide Nano-fillers for High Dielectric Mediums. Journal of Polymers and the Environment. 2020;28(9):2422-2432.
44. Hoque MA, Ahmed MR, Rahman GT, Rahman MT, Islam MA, Khan MA, et al. Fabrication and comparative study of magnetic Fe and α-Fe_2O_3 nanoparticles dispersed hybrid polymer (PVA + Chitosan) novel nanocomposite film. Results in Physics. 2018;10:434-443.
45. Hassan HB, Hasan AS, Hashim A. Synthesis and boosting the structural, optical and electronic characteristics of PS/SiC/In2O3 promising nanohybrid structures for tailored optoelectronics applications. Optical and Quantum Electronics. 2023;56(2).
46. Ali ZH, Hasan AS, Braihi AJ. Synthesis, Characterization, and Infrared Blocking Efficiency of Polyvinyl Alcohol Composites Filled with Cadmium Sulfide and Zinc Sulfide NPs. Ann Chim - Sci Mat. 2024;48(1):73-83.
47. Zatalini Df, Hendradi E, Philip D, Sari R. The Effect of Chitosan and Polyvinyl Alcohol Combination on Physical Characteristics and Mechanical Properties of Chitosan-PVA-Aloe vera Film. JURNAL FARMASI DAN ILMU KEFARMASIAN

INDONESIA. 2023;10(2):151-161.
48. Hassan HB, Hasan AS, Hashim A. Fabrication and advanced optical and electronic characteristics of PVA/SiC/CeO_2 hybrid nanostructures for augmented nanoelectronics and optics fields. Optical and Quantum Electronics. 2023;56(3).
49. Han X, Ge J, Luo J, Wang Y, Zhao X, Zhang F, et al. Construction of vacancies-enriched CuS/Fe_2O_3 with nano-heterojunctions as negative electrode for flexible solid-state supercapacitor. J Alloys Compd. 2022;916:165443.
50. Hasan AS, Hassan HB, Hashim A, Hasan NB, Al-kawaz YA. Modeling, Fabrication and Characteristics of Novel (PVA-SiC-In2O3) Nanohybrid Structures for Optoelectronic Applications. Silicon. 2024;16(9):4125-4138.
51. Hashim A, Hasan AS, Hadi A, Al-shujairi MA, Kadem ZA. Manufacturing and ameliorating the microstructure, optical, electronic and electrical features of (PVA-MC/CeO_2-SiO_2) multifunctional films for flexible optoelectronics applications. Ceram Int. 2025;51(30):62529-62539.
52. Hasan AS, Abbas MH, Hashim A, Jassem AE, Al-maamori MH, Khalid HM, et al. Ameliorating and Tuning the Microstructure, Electronic and Optical Features of PMMA-SiC-ZnO Futuristic Nanostructures for Tailored Nanoelectronics Applications. Silicon. 2025;17(9):2155-2169.
53. Widayat W, Arman MAP, Syarief E, Buchori L, Sulardjaka S. Sintesis, Karakterisasi dan Pengujian Katalis CaO-MgO/Fe_2O_3 dari Dolomit dan Pasir Besi untuk Pembuatan Biodiesel dari Minyak Goreng Bekas. TEKNIK. 2024;45(1):91-100.
54. Hasan AS, Hashim A, Khalid HM. Synthesis and Ameliorating the Features of PMMA/CdS-SiO_2 Futuristic Nanomaterials for Nanoelectronics and Optical Applications. Transactions on Electrical and Electronic Materials. 2025;26(5):713-727.
55. Dennis JO, Shukur MF, Aldaghri OA, Ibnaouf KH, Adam AA, Usman F, et al. A Review of Current Trends on Polyvinyl Alcohol (PVA)-Based Solid Polymer Electrolytes. Molecules. 2023;28(4):1781.
56. Hasan AS, Hashim A, Jassem AE, Al-maamori MH, Alkawaz YA, Alameer ZS. Tuning and Ameliorating the Microstructure and Electronic Features of SiC/PtSi Promising Nanostructures Doped Optical Material for Multifunctional Optoelectronics Applications. Silicon. 2025;17(9):2059-2069.
57. Hasan AS, Kadhim MJH, Hashim A, Jassem AE, Al-shujairi MA, Kadem ZA. Exploring the electronic, structural and optical features of SiS_2-LiF and SnS-SiBr4 new nanostructures doped PANI for optoelectronics and solar cells applications. Journal of Umm Al-Qura University for Applied Sciences. 2025.
58. Hadi A, Salman SR, Al Maimuri NML, Hashim A, Rashid FL, Hasan AS. Synthesis and Tailoring the Optimization and Dielectric Properties of PMMA/PEG/Barium Titanate Hybrid Nanostructures for Energy Storage and Electronics Applications. Chemistry and Chemical Technology. 2025;19(2):277-285.
59. Irmukhametova G, Al Azzam KM, Mun GA, Bekbayeva L, Dinara Z, Yermukhambetova BB, et al. Obtaining and Characterization of Biodegradable Polymer Blends Based on Polyvinyl Alcohol, Starch, and Chitosan. Polymers. 2025;17(4):479.

CC BY